

# Predictability in two-dimensional decaying turbulence

G. Boffetta

Dipartimento di Fisica Generale, Università di Torino, Via Pietro Giuria 1, 10125 Torino, Italy  
and INFM Sezione di Torino, Italy

A. Celani

Dipartimento di Ingegneria Aeronautica e Spaziale, Politecnico di Torino,  
C. Duca degli Abruzzi 24, 10129 Torino, Italy

A. Crisanti and A. Vulpiani

Dipartimento di Fisica, Università di Roma "La Sapienza," P.le Aldo Moro 2, 00185 Roma, Italy  
and INFM Sezione di Roma, Italy

(Received 21 February 1996; accepted 4 October 1996)

Predictability problem for two-dimensional decaying turbulence is addressed by means of numerical simulations. Qualitative and quantitative comparisons with previous results obtained by closure approximations are critically examined. It is found that, as for other features of two-dimensional turbulence, the role of coherent vortices is essential for a correct interpretation of the results. A Lagrangian, vortex-based, definition for the growth of uncertainties leads in general to an enhancement of the predictability time. © 1997 American Institute of Physics.  
[S1070-6631(97)00302-4]

## I. INTRODUCTION

A problem with an obvious interest in many fields, e.g., weather forecasting, is the prediction of the future state of a system once known the evolution laws and the initial conditions.<sup>1</sup> It is now part of the folklore of chaos that predictability in the presence of deterministic chaos has severe limitations because of the exponential divergence of the distance between two initially close trajectories.

Typically one has that an uncertainty  $\delta\mathbf{x}(0)$  on the state of the system at time  $t=0$  increases as

$$|\delta\mathbf{x}(t)| \approx |\delta\mathbf{x}(0)|e^{\lambda t}, \quad (1)$$

where  $\lambda$  is the maximum Lyapunov exponent<sup>2</sup>. If one accepts a tolerance  $\delta_{\max}$  on the predicted state of the system, then Eq. (1) implies that a system can be considered predictable up to the *predictability time*

$$T_p \sim \frac{1}{\lambda} \ln \left( \frac{\delta_{\max}}{\delta_0} \right), \quad (2)$$

where  $\delta_0 = |\delta\mathbf{x}(0)|$ .

Relation (2) tells us that the predictability time, if one considers *infinitesimal perturbations*, is basically proportional to the inverse of the Lyapunov exponent since the dependence on the precision of the measure and the threshold is very weak (logarithmic).

However Eq. (2) is a very naive answer to the predictability problem and its validity is very limited since it does not take into account some important features of chaotic systems.

The main reasons for the failure of Eq. (2) can be summarized as follows:

(a) The Lyapunov exponent  $\lambda$  is a global quantity. It measures the *average* exponential rate of divergence of nearby trajectories. In general there exist finite-time fluctuations of this rate and it is possible to define an "instantaneous" rate  $\gamma_i(\tau)$ , the effective Lyapunov

exponent, which depends on the particular point of the trajectory  $\mathbf{x}(t)$  where the perturbation is performed and on the time delay  $\tau$  from the perturbation.<sup>3</sup> Therefore the predictability time  $T_p$  fluctuates, following the  $\gamma$  variations.<sup>4,5</sup>

(b) In dynamical systems with many degrees of freedom, the interactions among different parts of the system can play an important role in the growth of perturbations. In addition, one is often interested in the case of perturbations concentrated on certain degrees of freedom while the prediction is on the evolution of other degrees of freedom. For example in weather forecasting the uncertainties are on small scales while predictions are on large scales. Therefore the mechanism of the transfer of the error through the different degrees of freedom of the system could be more important than the rate of divergence of nearby trajectories.<sup>6</sup>

(c) In systems with many characteristic times, such as the eddy turnover times in fully developed turbulence, if the perturbations are not infinitesimal or if the threshold of accepted error is not small,  $T_p$  is determined by the detailed mechanism of the dynamics due to the nonlinear effects in the evolution equation for  $\delta\mathbf{x}$ . In this case, the predictability time could have no relation with the maximum Lyapunov exponent and  $T_p$  depends in a non-trivial way on the system.<sup>7,8</sup>

(d) Even at very high Reynolds number, there exist well defined coherent structures, such as vortex tubes, which roughly move maintaining their shape. In this case, if one is interested only in some qualitative behaviors, one should reformulate the predictability problem. For instance, a reasonable question is the prediction of the center and the orientation of the vortex tubes. In this case one could hope to have a long predictability time.

In this paper we study the predictability problem in two-

dimensional (2D) incompressible turbulence by means of numerical simulations by using both infinitesimal and finite perturbations on the initial condition.

Section II is a brief summary of the classical results on predictability in 2D turbulence. Section III contains the description of the numerical simulations performed and the comparison with the classical results. A Lagrangian, vortex-based, measure for the predictability is introduced and discussed in Sec. IV. Section V is devoted to some conclusions. Finally, the Appendix contains a simple vortex model which links the Lagrangian and Eulerian pictures of the error growth.

## II. BRIEF SUMMARY OF PREVIOUS RESULTS

The first attempt to study the predictability problem in turbulence from an analytical point of view was done by Leith and Kraichnan.<sup>9,10</sup> Making use of different closure approximations as the eddy damped quasi normal Markovian (EDQNM) or test field model (TFM) on the Navier–Stokes equations, they examined the error growth both in the energy and enstrophy cascade in three- and two-dimensional turbulence. Their fundamental papers become the backbone for more recent approaches developed in recent years.<sup>11</sup> For completeness we recall here the main results obtained by closure approximations.

Given two realizations of the velocity field  $\mathbf{u}^{(1)}(\mathbf{x}, t)$  and  $\mathbf{u}^{(2)}(\mathbf{x}, t)$ , a suitable measure for the predictability is the error field

$$\delta\mathbf{u}(\mathbf{x}, t) = \frac{1}{\sqrt{2}}(\mathbf{u}^{(2)}(\mathbf{x}, t) - \mathbf{u}^{(1)}(\mathbf{x}, t)) \quad (3)$$

from which we define the error energy and error enstrophy

$$E_{\Delta}(t) = \frac{1}{2} \langle |\delta\mathbf{u}(\mathbf{x}, t)|^2 \rangle = \int_0^{\infty} E_{\Delta}(k, t) dk, \quad (4)$$

$$Z_{\Delta}(t) = \frac{1}{2} \langle |\nabla \times \delta\mathbf{u}(\mathbf{x}, t)|^2 \rangle = \int_0^{\infty} k^2 E_{\Delta}(k, t) dk. \quad (5)$$

We assume that the two realizations are equivalent in the sense that they have the same energy  $E(k, t)$  and enstrophy  $Z(k, t) = k^2 E(k, t)$  spectrum. The normalization in (3) is chosen in order to obtain the saturation to the mean energy and mean enstrophy

$$E_{\Delta} \rightarrow E = \frac{1}{2} \langle |\mathbf{u}^{(1)}|^2 \rangle = \frac{1}{2} \langle |\mathbf{u}^{(2)}|^2 \rangle, \quad (6)$$

$$Z_{\Delta} \rightarrow Z = \frac{1}{2} \langle |\nabla \times \mathbf{u}^{(1)}|^2 \rangle = \frac{1}{2} \langle |\nabla \times \mathbf{u}^{(2)}|^2 \rangle, \quad (7)$$

for completely uncorrelated velocity fields.

The initial error is usually chosen to be confined at small scales, i.e.,  $E_{\Delta}(k, 0) = 0$  and  $Z_{\Delta}(k, 0) = 0$  for  $k < k_0$ , an assumption physically justified by the finite resolution of any measurement device and/or numerical simulation scheme. Due to the non-linear coupling of different scales, the error spreads to invade the larger, physically relevant, scales with a process which eventually overpowers the dissipation of the error by viscosity. In closure approximations it found that the growth of the relative error spectrum

$$r(k, t) = \frac{E_{\Delta}(k, t)}{E(k, t)} = \frac{Z_{\Delta}(k, t)}{Z(k, t)} \quad (8)$$

is almost independent of the particular form of the initial error spectrum  $E_{\Delta}(k, 0)$  and  $Z_{\Delta}(k, 0)$ .

The error transfer towards large scale can be quantified by the characteristic wavenumber  $k_E(t)$  at which the error spectrum is a given fraction of the reference spectrum. Leith and Kraichnan,<sup>10</sup> defining  $k_E$  such that  $r(k_E) = 0.5$ , found a stationary similarity error spectrum  $r(k/k_E)$  in which the time dependence is only through  $k_E(t)$ . The predictability time  $T_p$  is finally defined in terms of the global relative error energy

$$r(t) = \frac{E_{\Delta}(t)}{E(t)} \quad (9)$$

by the condition  $r(T_p) = 1/4$ .

For an initial spectrum confined above a (large) wave vector scale  $k_0$ , lying in the enstrophy inertial range, the time necessary for a scale  $k < k_0$  to be affected is logarithmic in  $k_0/k$ , hence the predictability of two-dimensional turbulence increases without bound with the initial resolution ( $k_0 \rightarrow \infty$ ). This scenario is very different from what is found for three-dimensional turbulence, where the time for the transfer of error between different scales is essentially given by the characteristic time of the largest scale involved and hence independent of the distance on the energy cascade.

The dependence of the predictability time on the error injection scale  $k_0$  can be understood by dimensional analysis, according to which the eddy turnover time is constant in the direct enstrophy cascade. The time for a scale  $k$  to be affected by a perturbation initially located at scale  $k_0 = 2^n k$  is in fact proportional to number of steps  $n$  in the cascade.

## III. NUMERICAL SIMULATIONS

The model equation for the study of two-dimensional turbulence is the incompressible vorticity equation with generalized dissipation<sup>12,13</sup>

$$\frac{\partial \omega}{\partial t} + \frac{\partial(\psi, \omega)}{\partial(x, y)} = (-1)^{p+1} \nu_p \Delta^p \omega \quad (10)$$

in which  $p$  is the order of the dissipation,  $p = 1$  for ordinary dissipation,  $p > 1$  for superviscosity or hyperviscosity. The quantity  $\omega$  is the vorticity field and  $\psi$  is the stream function given by  $\Delta \psi = -\omega$ .

The numerical method adopted is the standard pseudo-spectral,<sup>15</sup> dealiased code<sup>16</sup> with a second-order Adams–Bashforth time step integrator. The computational domain is the  $N \times N$  square with side  $L = 2\pi$  and periodic boundary conditions.

For the numerical simulations we will adopt the hyperviscous version of (10) ( $p = 4$ ), although it has been demonstrated that it is not completely equivalent to the standard Navier–Stokes equation ( $p = 1$ ), especially for what concerns the small scale features of the vorticity field.<sup>14</sup> Nevertheless these differences do not affect the content of the present paper, that is the comparison of different norms for the error field within a given model (i.e., a given  $p$ ).

The initial condition, generated in spectral space with an initial energy spectrum  $E_0(k)$  and random phases, is integrated for a sufficiently long time in order to generate coherent structures. The so obtained field configuration is taken as the new initial configuration on which we make the perturbations, and the time is set to  $t=0$ .

The perturbed field is obtained from the reference field by either randomizing the phase of the Fourier components above a given wavenumber  $k_0$ , or by adding some noise of strength  $\epsilon$  in parts or in the whole physical space. In most simulation we used the first kind of perturbation in order to simulate finite resolution knowledge.<sup>9</sup> However, we have found that the perturbation growth is independent of the initial form of the small perturbation.

The two fields, the reference  $\omega$  and the perturbed  $\omega'$ , are integrated independently for a total time  $t_{\text{tot}}$  and sampled every time interval  $\Delta t$  for analysis purposes.

The local error field is defined following (3) as

$$\delta\omega(\mathbf{x},t) = \frac{1}{\sqrt{2}}(\omega'(\mathbf{x},t) - \omega(\mathbf{x},t)) \quad (11)$$

from which the error enstrophy and energy are obtained as

$$Z_{\Delta}(t) = \int_0^{\infty} dk Z_{\Delta}(k,t) = \frac{1}{2} \int d^2x |\delta\omega(\mathbf{x},t)|^2, \quad (12)$$

$$E_{\Delta}(t) = \int_0^{\infty} dk E_{\Delta}(k,t) = \int_0^{\infty} dk k^{-2} Z_{\Delta}(k,t). \quad (13)$$

The relative total energy and enstrophy error are defined as

$$r(t) = \frac{E_{\Delta}(t)}{E(t)}, \quad z(t) = \frac{Z_{\Delta}(t)}{Z(t)}. \quad (14)$$

The fractions  $r(t)$  and  $z(t)$  give a global measure of the error varying between 0 for no error and 1 for error saturation.

The method used for defining the distance between the reference and perturbed field can be a delicate point for a high dimensional system like direct simulation of Navier–Stokes equation. This issue was already addressed in Ref. 17 where the infinitesimal (linear) error growth was computed using several Eulerian norms. By Eulerian norm we mean the average of a local measure in the error field, such as the enstrophy of the error field. Our approach is different because we are interested mainly in finite perturbations and simulations are performed until the error saturates and the reference and perturbed field are completely uncorrelated. As for Eulerian norms the decorrelation time in principle depends on the distance used, moreover we shall see in the next section that due to the presence of coherent structures a Lagrangian measure, i.e., based on the position of coherent structures, should be more appropriate.<sup>18</sup>

For infinitesimal perturbation, the error is expected to grow exponentially as  $r(t) \approx r(0)\exp(2\lambda t)$ . The largest Lyapunov exponent  $\lambda$  is an asymptotic quantity of the system. We are dealing with a dissipative system which ultimately collapses on the trivial fixed point  $\omega=0$ , therefore from a mathematical point of view  $\lambda$  is negative. For non-stationary systems it is thus more physical to introduce the

TABLE I. Parameters for the simulation:  $N$ : resolution;  $p$ : order of the hyperviscosity;  $\nu_p$ : generalized viscosity;  $E_0(k)$ : initial energy spectrum;  $E$ : total energy;  $Z$ : total enstrophy;  $\tau_0$ : eddy turnover time;  $\Delta t$ : sampling time;  $t_{\text{tot}}$ : total simulation time;  $E_{\Delta}$ : energy of the error field;  $Z_{\Delta}$ : enstrophy of the error field.

| $N$               | 256                    | 512                     |
|-------------------|------------------------|-------------------------|
| $p$               | 4                      | 4                       |
| $\nu_p$           | $10^{-14}$             | $10^{-16}$              |
| $E_0(k)$          | $k^{-3}\theta(k-20)$   | $k^{-3}\theta(k-40)$    |
| $E(t=0)$          | 0.078                  | 0.017                   |
| $Z(t=0)$          | 4.12                   | 1.74                    |
| $\tau_0$          | 2.2                    | 3.4                     |
| $\Delta t$        | 2.0                    | 4.0                     |
| $t_{\text{tot}}$  | 300.0                  | 500.0                   |
| Initial error     | random phase, $k_0=60$ | random phase, $k_0=120$ |
| $E_{\Delta}(t=0)$ | $2.5 \times 10^{-7}$   | $2.1 \times 10^{-10}$   |
| $Z_{\Delta}(t=0)$ | $9.8 \times 10^{-4}$   | $3.2 \times 10^{-6}$    |

effective Lyapunov exponent  $\gamma_{\tau}(t)$  which measures the average divergence of close trajectories over a given time interval  $\tau$ :

$$\gamma_{\tau}(t) = \frac{1}{2\tau} \log \frac{r(t+\tau)}{r(t)}. \quad (15)$$

The Lyapunov exponent is recovered by taking the limit  $r(t) \rightarrow 0$  and  $\tau \rightarrow \infty$ .

The effective Lyapunov exponent computed in our simulation shows a very little, if any, dependence on  $t$  due to the fact that the viscous dissipation time scale is much longer than simulation time  $t_{\text{tot}}$ . Thus  $\gamma_{t_{\text{tot}}}(0)$  can be taken as the Lyapunov exponent for decaying turbulence simulations.

The exponential error growth regime lasts until the separation of the two fields cannot be considered any more infinitesimal and a second regime sets in. Here the time evolution is no more universal and depends on the system details. This regime, nevertheless, can be more relevant to characterize the predictability time defined through finite, rather than infinitesimal, errors.<sup>8</sup>

Several numerical experiments performed with different resolution, initial conditions and perturbations, show a generic picture which will be discussed in detail for two simulations at different resolutions whose parameters are summarized in Table I.

The results for the simulation at lower resolution ( $N=256$ ) are averaged over four different realizations of the perturbed field. In Fig. 1(a) we report the evolution of  $r(t)$  and  $z(t)$  in a linear-log plot. The choice of the threshold  $r(T_p)=0.25$  gives a predictability time  $T_p=177 \sim 80\tau_0$ , where  $\tau_0$  is the eddy turnover time. From Fig. 1(a) we see that for small times both  $r(t)$  and  $z(t)$  have an exponential growth with growing rate  $\sim 0.14$ , corresponding to an effective Lyapunov exponent  $\gamma \sim 0.07$ . At later times,  $t > 80$ , the error curves bend since the error cannot be considered anymore infinitesimal. Observe that about half of the predictability time  $T_p$  is governed by non-infinitesimal error growth behavior. Thus, as already demonstrated in several papers,<sup>4-7</sup> the predictability time is an independent measure of the error

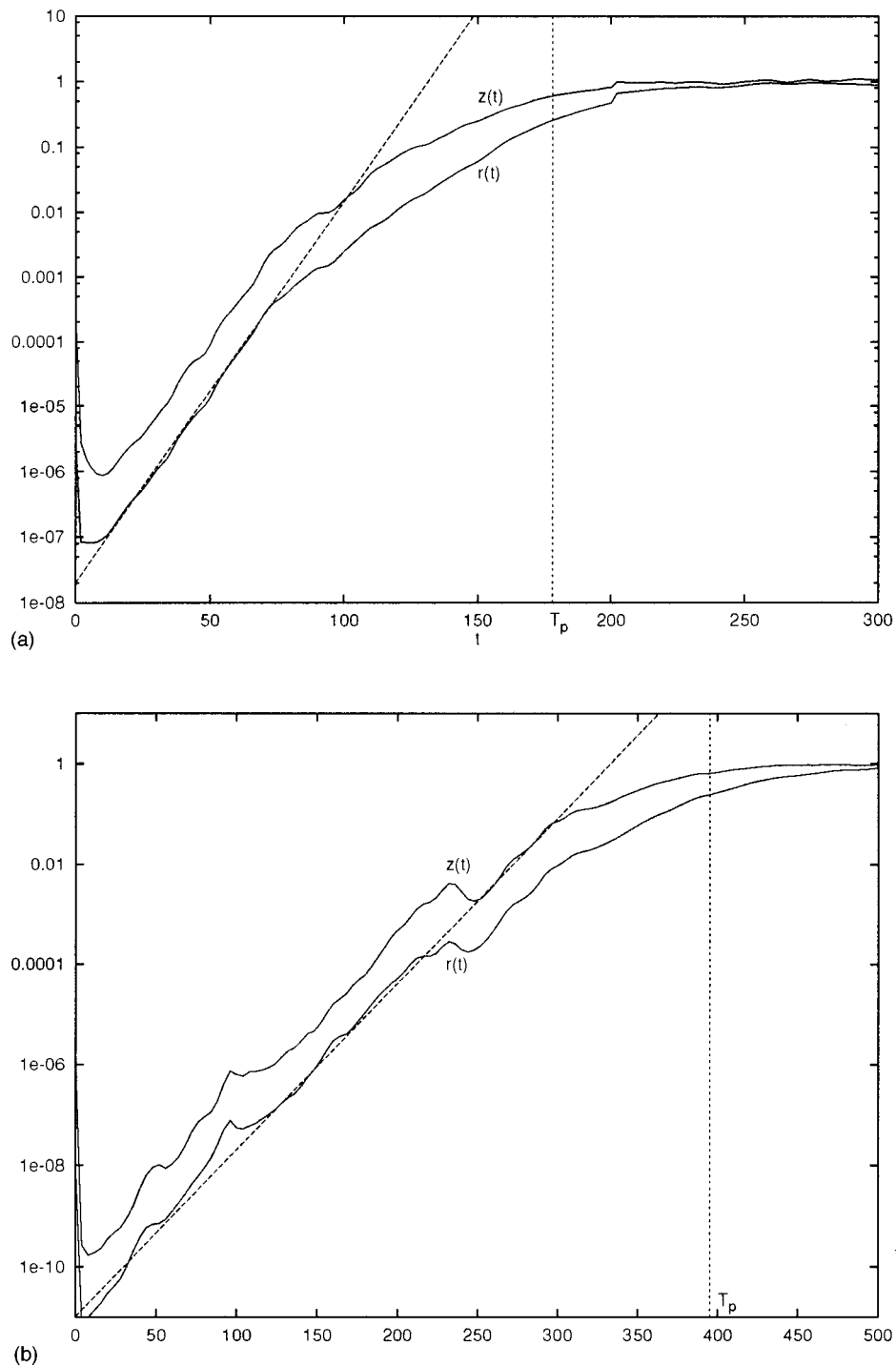


FIG. 1. Relative energy ( $r$ ) and enstrophy ( $z$ ) error growth for (a)  $N=256$  and (b)  $N=512$  simulations.  $T_p$  indicates predictability times defined as  $r(T_p)=0.25$ . The dashed lines represent the exponential regimes with  $r(t)\sim\exp(0.14t)$  and  $r(t)\sim\exp(0.08t)$  respectively.

growth in a chaotic system. It can be completely unrelated with the Lyapunov exponent and, in principle, it may depend on the initial condition and initial error.

In Fig. 1(a) we also observe a decrease of the global error at very small times. This effect is due to the dissipation which removes enstrophy and energy from the smallest uncorrelated scales which are filled by larger, correlated, scales. The effect lasts until it is overpowered by the error spreading to larger scales which decorrelates the two field. This effect was already observed and discussed in Ref. 10. A simulation

performed without viscosity showed no initial decreasing in the error functions.

Figure 1(b) shows the analogous result for the  $N=512$  simulation. The predictability time here is longer,  $T_p=395$ , due to smaller initial error and slower dynamics.

Vorticity-based measure  $z(t)$  or energy-based measure  $r(t)$  give the same qualitative behavior, upon an almost constant rescaling. The enstrophy error is always larger than the energy error reflecting the fact that the former emphasizes the smaller scales on which the error is initially injected. The

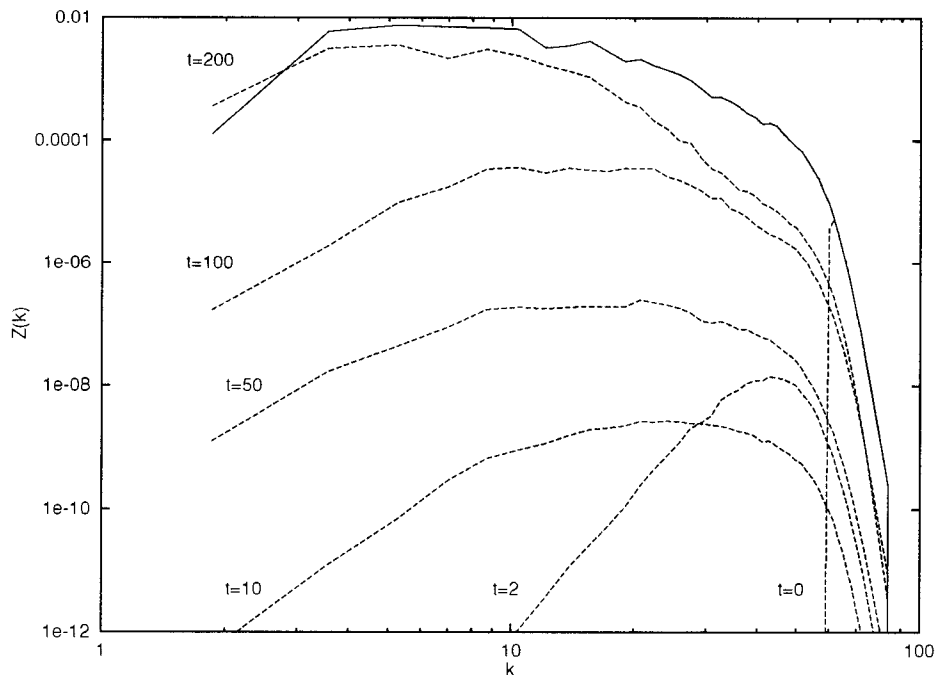


FIG. 2. Enstrophy spectrum  $Z(k)$  at  $t=0$  for the  $N=256$  simulation. Dashed lines: enstrophy error spectra  $Z_{\Delta}(k,t)$  at different times. The perturbed field at  $t=0$  is obtained by randomizing the Fourier phases for  $k>60$ .

fact that  $z(t)$  saturates before  $r(t)$  suggest that large scales are the last scales that decorrelate.

This effect can be investigated more in detail by looking at the enstrophy error spectrum  $Z_{\Delta}(k,t)$  plotted in Fig. 2 for different times. For comparison in Fig. 2 is also reported the (non-stationary) reference enstrophy spectrum  $Z(k,0)$  at the initial time. As expected the error transfers to larger and larger scales, again in qualitative agreement with the closure computations.

#### IV. ERROR GROWTH AND VORTEX DYNAMICS

It is well known that decaying 2D turbulence is characterized by the presence of coherent vortex structures which dominate the dynamics in the field.<sup>12,13</sup> The error measure based on the spectra, either of the error energy or of the error enstrophy, described in the previous section neglects the spatial details of the field since all phase correlations are lost. A closer look at the difference field reveals that it is concentrated mainly within the vortices. This is because a small displacement of two vortices gives a large difference field. For example in Fig. 3 it is shown the reference and the perturbed vorticity field at the predictability time  $T_p$  for the  $N=256$  simulation. Although at  $T_p$  we have, by definition, 25% of energy error and about 65% of enstrophy error, the two fields are remarkably similar for what concerns vortex populations. Most of the large coherent structures are present in both fields in almost the same positions. Only the background and the smallest vortices seem to be completely uncorrelated. Figure 3 also shows the difference field  $\delta\omega(\mathbf{x})$  at time  $T_p$ . The error is concentrated within the vortices in a typical bipolar configuration already observed in previous

simulations.<sup>17,19</sup> It is therefore natural to address the problem of predictability from the point of view of vortex motion<sup>18</sup> rather than in the spectral space, where no universal behavior is known, at least at finite Reynolds numbers.

Vortex dynamics is well approximated by a conservative dynamics in which each vortex carries its own vorticity and moves according to the point vortex Hamiltonian system. Dissipation effects take place mostly during merging processes, a local inelastic collision in which two close, equal sign, vortices merge to form a single larger vortex. Some vorticity is released during the collision and rapidly dissipated. Vortex merging do not seem to be a simple, universal, vortex interaction, although it can be approximatively described in terms of energy conservation laws.<sup>20-22</sup>

Straining process is the other mechanism for vortex dissipation. Straining is a kind of failed vortex merging in which one of the interacting vortices is stretched rapidly and completely dissipated. Straining is observed to be more likely for interactions between vortices different in size, the smaller vortex being destroyed by the larger one, while merging seems to be the favorite in interactions between almost equal vortices.

In freely decaying turbulence, vortex population  $N_v(t)$  decays as a consequence of vortex interactions, until a final state with a single dipole ( $N_v=2$ ) survives over a long dissipative time scale.<sup>23</sup>

For studying in detail vortex features, we employed a *vortex tracking* algorithm which recognizes and follows vortices during the simulation evolution. The algorithm defines a vortex as a connected region  $D_{\alpha}$  in the computational domain. Vortex domains  $D_{\alpha}$  are defined as follows: a local

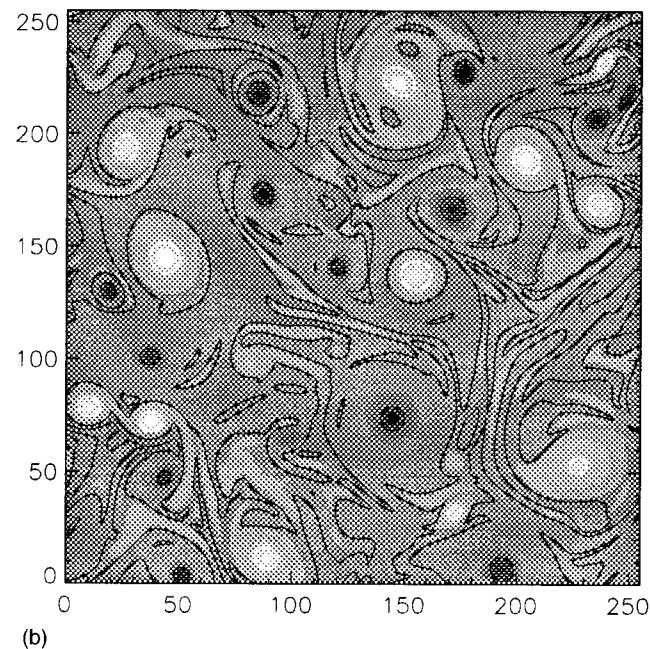
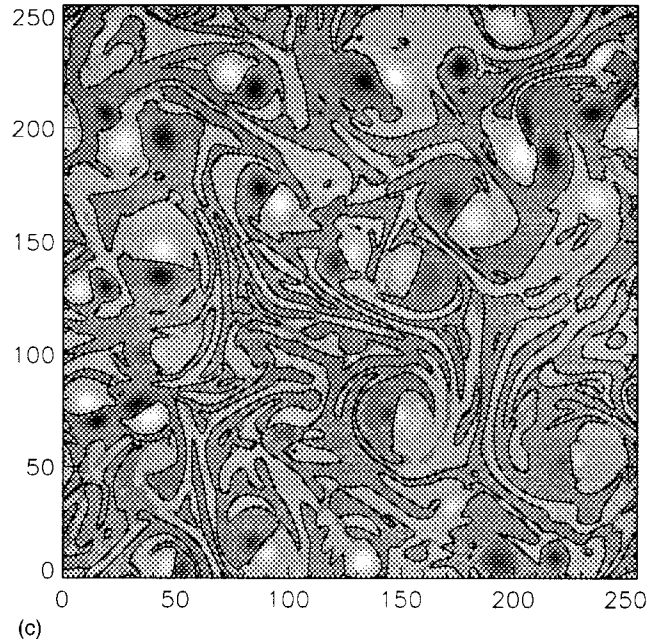
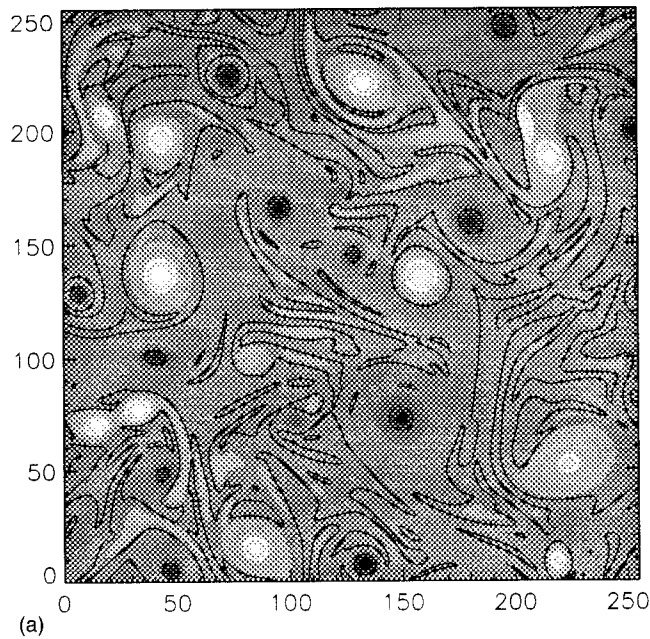


FIG. 3. Gray-scale map of the vorticity fields ( $N=256$ ) at time  $T_p=177$ . White corresponds to positive vorticity regions, black to negative ones. (a) Reference field  $\omega(\mathbf{x})$ . (b) Perturbed field  $\omega'(\mathbf{x})$ . (c) Error field  $\delta\omega(\mathbf{x})$ .

vorticity extremum  $z_\alpha$  (vorticity peak) whose value must be greater (in absolute value) than a given global threshold; all the connected grid cells whose vorticity is (in absolute value) greater than a given fraction ( $\epsilon=0.2$ ) of the vorticity peak. Given the vortex domains  $D_\alpha$ , all the physical vortex quantities are computed by integrating inside the domains. Finally, vortex trajectories are reconstructed by matching peak positions at different times.

Most of the vortices experience several inelastic interactions during the simulation time. At the beginning of the simulation, vortex tracking algorithm find  $N_v(0)=73$  vortices, while at the end only  $N_v(200)=23$  remain. Of the initial vortices, 51 merged one or more times, 6 survived without interactions and the last 16 were destroyed by straining mechanism. Vortices carry most of the enstrophy of the field:

about 82% at  $t=0$  and 92% at  $t=200$ . About 55.7% of the initial enstrophy is dissipated during the simulation: 45.2% by vortices which merged, 7.9% is lost in straining processes and the remaining 2.6% is dissipated by vortices which do not interact.

To emphasize the limits of the Eulerian measure for the error (4,5), consider the case of a vorticity field made of small blobs (vortices). It is easy to realize that a displacement in the positions of the blobs which is comparable with their size is sufficient to achieve the saturation of the error. Thus a definition of predictability based on Eulerian measure reveals to be dependent on the vortex size. In general we expect that, in presence of vortices, an Eulerian based measure underestimates the predictability time. In the limiting case of singular point vortices, for example, an infinitesimal

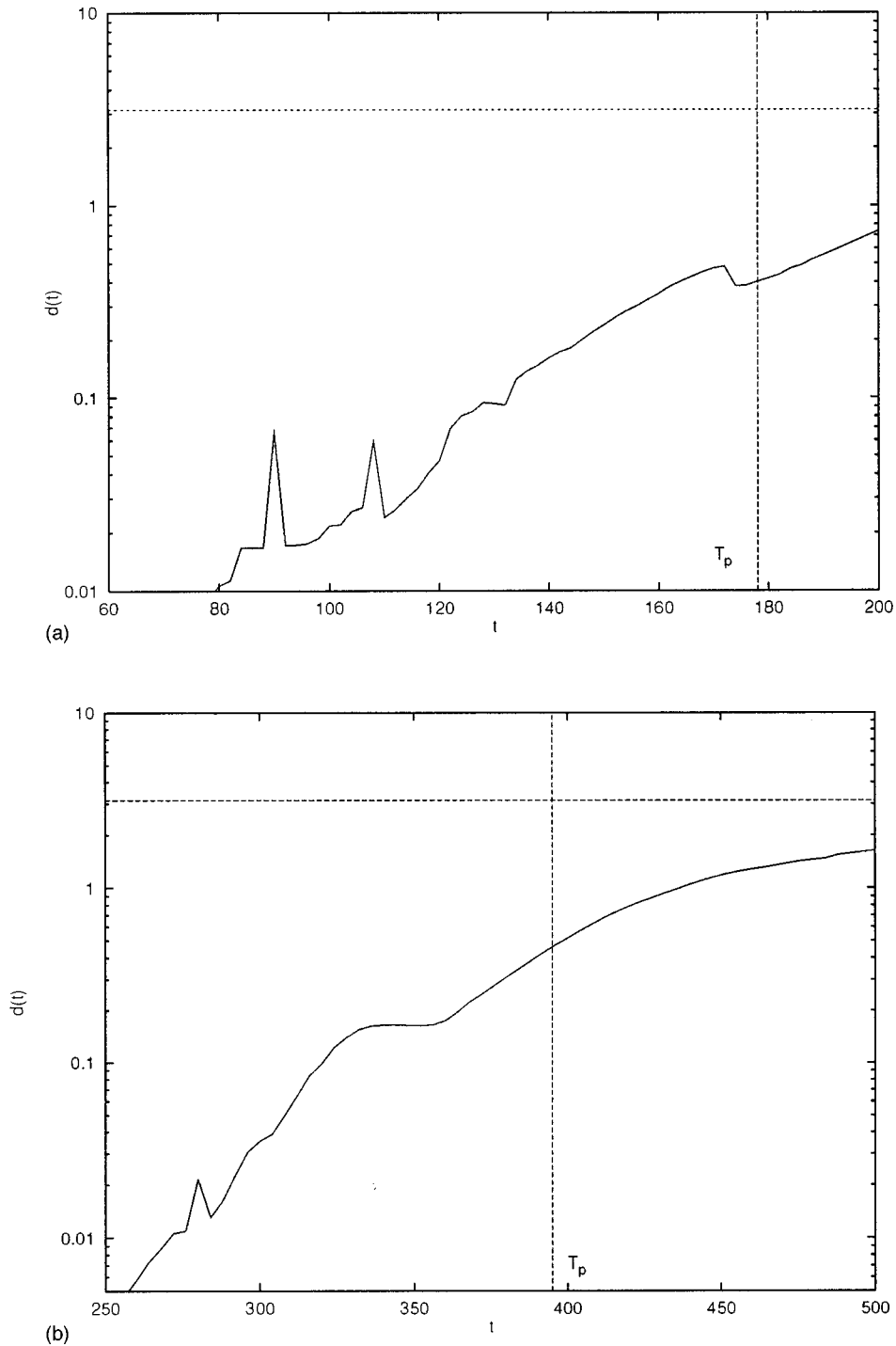


FIG. 4. Mean vortex separation  $d(t)$ . (a) Resolution  $N=256$ . For times  $t < 150$  the mean separation is below the resolution  $\delta x = 2\pi/N \sim 0.24$  on the grid. Observe that at the classical predictability time  $T_p \sim 177$ , the separation  $d(T_p)$  is about one-tenth of the saturation level (dashed line). (b) Resolution  $N=512$ .

error in the coordinates gives error saturation and hence zero predictability time. This problem can be overcome by resorting to the natural Euclidean distance in the point vortices phase space.

Following this analysis, in the case of decaying two-dimensional turbulence (i.e., a flow whose dynamics is ruled by vortices), it looks sensible to introduce a Lagrangian based measure defined as

$$d^2(t) = \frac{1}{\sum_{\alpha} |\Gamma_{\alpha}|} \sum_{\alpha} |\Gamma_{\alpha}| (\mathbf{x}'_{\alpha} - \mathbf{x}_{\alpha})^2, \quad (16)$$

where  $\mathbf{x}_{\alpha}$  and  $\mathbf{x}'_{\alpha}$  are the coordinates of the two vortex populations and the weights  $\Gamma_{\alpha}$  are the vortex circulations

$$\Gamma_{\alpha} = \int_{D_{\alpha}} d^2x \omega(\mathbf{x}). \quad (17)$$

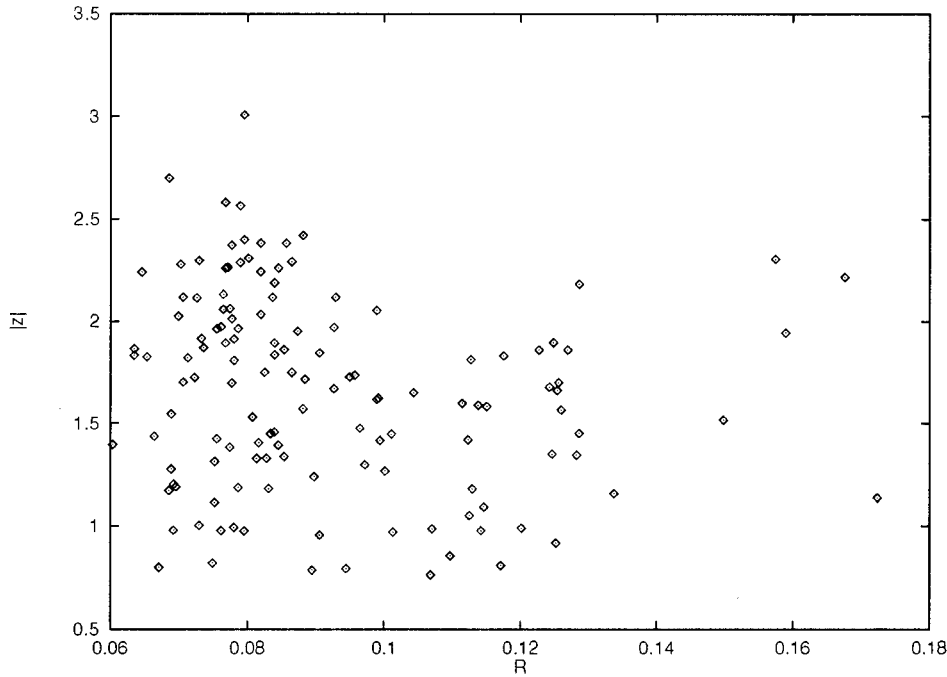


FIG. 5. Vorticity peak absolute values versus vortex radii for the largest 133 vortices found in the  $N=512$  simulation. Observe the absence of correlations and the rather large distribution of vortex population.

This is nothing that one of the possible choices that can be made; in the appendix another Lagrangian measure arises considering a field of isolated vortices.

In Fig. 4(a) we observe that at the classical predictability time the mean vortex separation is  $d(T_p)=0.40$ , well below the saturation value  $d_{\max}\sim L/2=\pi$ . This result seems to be independent on the resolution, as is shown in Fig. 4b relative to the  $N=512$  simulation. Also in this case the mean vortex separation at the predictability time  $d(T_p)=0.45$  is well below the saturation value.

We emphasize that the Lagrangian measure  $d(t)$  and the Eulerian measure  $r(t)$  of the error growth give different answers for the error level, and hence for the predictability time, defined as the time at which the error reaches a given threshold, but they do not give different error growth laws, at least for small times where the error is infinitesimal and grows exponentially with the largest Lyapunov exponent.

These considerations seem to be insensitive to the resolution at which the simulations are performed, as is clearly shown in Fig. 4. We think that the  $N=512$  simulation has high enough resolution for our purposes since in this case we observe a widespread distribution of vortex features. This is shown in Fig. 5 where the absolute value of the vorticity peaks versus the vortex radii are plotted for the 133 larger vortices.

## V. CONCLUSIONS

We numerically investigated the predictability problem for two-dimensional decaying turbulence. A generic definition of predictability time requires two ingredients: a measure of relative error between the reference and the perturbed field and a threshold value for this quantity.

Within the limits of Eulerian based definitions for the error, e.g., average energy or enstrophy of the error field, predictability time estimates look quite similar and in qualitative agreement with closure approximations.

We have shown that the Eulerian error growth is ruled by the error in the positions of vortices (see the Appendix); we have thus chosen this latter measure to define a Lagrangian based predictability time. With this definition we observed an enhanced predictability which seems to be insensitive to the initial (small) error and to the numerical resolution.

We stress that our results apply whenever the flow displays strong and long lived coherent structures and they could be relevant for characterizing the predictability in many geophysical flows.

## ACKNOWLEDGMENTS

G. B. and A. C. thank the ‘‘Istituto di Cosmogeofisica del CNR,’’ Torino, for hospitality and support. We also thank A. Provenzale for useful discussions. This work has been partially supported by the CNR research project ‘‘Climate Variability and Predictability.’’

## APPENDIX: A SIMPLE VORTEX MODEL FOR ERROR GROWTH

Here we introduce a simple vortex model, similar to the one described in Ref. 21, for linking the Eulerian error growth to vortex dynamics. Let us consider a two-dimensional vorticity field given by the superposition of  $N_v$  vortices. Each vortex is characterized by a vorticity distribution parametrized by the position  $\mathbf{x}_\alpha$  of the center, the vorticity peak  $z_\alpha(t)$  and the radius  $R_\alpha(t)$  (defined as the dis-



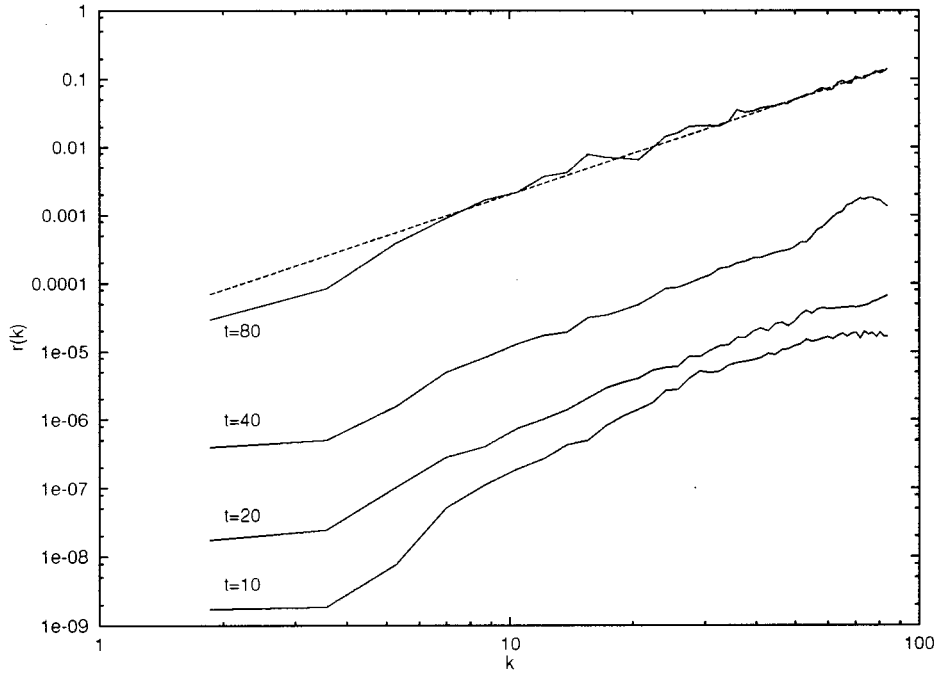


FIG. 6. Relative spectrum at small times for simulations at  $N=256$ . The dashed line is the prediction  $r(k) \sim k^{-2}$ .

tance from the center at which the vorticity has a fraction  $\epsilon$  of the peak value). The axisymmetric vortex shape is specified by a function  $f(r)$  constrained between the values  $f(0)=1$  and  $f(1)=\epsilon$ . We also assume no background, i.e.,  $f(r)=0$  for  $r>1$ . The vorticity field is thus given by

$$\omega_v(\mathbf{x}) = \sum_{\alpha} z_{\alpha} f\left(\frac{|\mathbf{x} - \mathbf{x}_{\alpha}|}{R_{\alpha}}\right). \quad (\text{A1})$$

Assuming two vortex populations obtained one from the other by a displacement  $\mathbf{d}_{\alpha}$  of each vortex  $\alpha$ , the error field is

$$\delta\omega_v(\mathbf{x}) = \frac{1}{\sqrt{2}} \sum_{\alpha} z_{\alpha} \left[ f\left(\frac{|\mathbf{x} - \mathbf{x}_{\alpha}|}{R_{\alpha}}\right) - f\left(\frac{|\mathbf{x} - \mathbf{x}_{\alpha} - \mathbf{d}_{\alpha}|}{R_{\alpha}}\right) \right]. \quad (\text{A2})$$

The enstrophy spectrum is obtained from the Fourier components  $\omega_v(\mathbf{k})$  of the vorticity field

$$Z(k) = \int |\omega_v(\mathbf{k})|^2 d\theta_k. \quad (\text{A3})$$

Assuming that the distance between two vortices is much larger than their radii, i.e., for a non-overlapping vortex field, we can write

$$Z(k) = k \sum_{\alpha} z_{\alpha}^2 R_{\alpha}^4 |\hat{f}(R_{\alpha}k)|^2, \quad (\text{A4})$$

where  $\hat{f}(k)$  is the Fourier transform of the vortex shape  $f(r)$ .

Under the same assumption, the error enstrophy spectrum becomes

$$Z_{\Delta}(k) = k \sum_{\alpha} z_{\alpha}^2 R_{\alpha}^4 |\hat{f}(R_{\alpha}k)|^2 (1 - J_0(d_{\alpha}k)), \quad (\text{A5})$$

where  $J_0(x)$  is the 0th-order Bessel function.

Assuming that the vortices are well localized structures, we have  $\hat{f}(R_{\alpha}k) \sim \text{const.}$  for small  $k$  ( $k < 1/R_{\alpha}$ ). For not too large separations,  $d_{\alpha}k \ll 1$ , we can approximate the Bessel function with  $J_0(x) \sim 1 - x^2/4$ . Then the relative spectrum  $r(k) = Z_{\Delta}(k)/Z(k)$  can be written, in first approximation, as

$$r(k) \sim \frac{1}{4} k^2 \langle d^2 \rangle, \quad (\text{A6})$$

where the average square separation is taken with weights  $z_{\alpha}^2 R_{\alpha}^4$ .

The vortex model leads to  $k^2$  behavior for the relative spectrum for short time and small  $k$ , which is effectively found in simulations, as shown in Fig. 6.

Within this model it is possible to compute the global relative enstrophy error  $z(t)$  by integrating (A4) and (A5) on wavenumber  $k$ . An explicit form can be obtained in the case of Gaussian vortices  $f(r) = e^{-r^2/2\ln\epsilon}$ :

$$z_v(t) = \frac{\sum_{\alpha} z_{\alpha}^2 R_{\alpha}^2 [1 - \exp(d_{\alpha}^2 \ln \epsilon / 2R_{\alpha}^2)]}{\sum_{\alpha} z_{\alpha}^2 R_{\alpha}^2} \quad (\text{A7})$$

which is plotted in Fig. 7. The good agreement with the global relative error  $z(t)$  (14) shows again that vortex pair separations  $d_{\alpha}$  rule the error growth in two-dimensional turbulence.

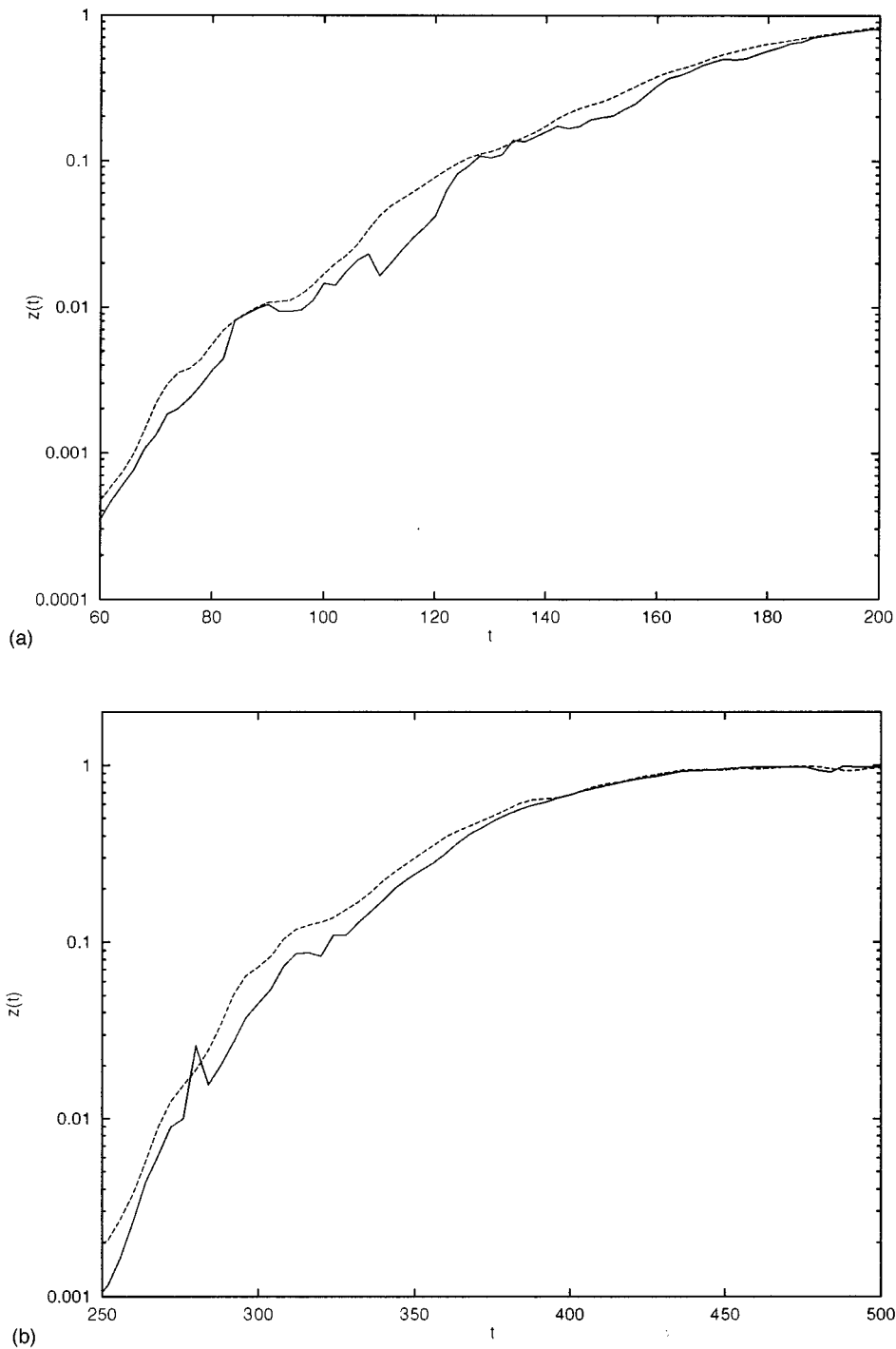


FIG. 7. Relative enstrophy error  $z_v(t)$  computed from the biggest vortices with Gaussian approximation. (a) Resolution  $N=256$ ; the number of vortices varies from 73 at  $t=0$  down to 23 at  $t=200$ . (b) Resolution  $N=512$ . For comparison, the global enstrophy relative error is also shown (dashed line).

<sup>1</sup>E. N. Lorenz, "The predictability of a flow which possesses many scale of motion," *Tellus* **21**, 289 (1969).

<sup>2</sup>G. Benettin, L. Galgani, A. Giorgilli, and J. M. Strelcyn, "Lyapunov characteristic exponents for smooth dynamical systems and Hamiltonian systems; a method for computing all of them. Part 1: Theory," *Meccanica* **15**, 9 (1980); "Lyapunov characteristic exponents for smooth dynamical systems and Hamiltonian systems; a method for computing all of them. Part 2: Numerical Application," *Meccanica* **15**, 20 (1980).

<sup>3</sup>G. Paladin and A. Vulpiani, "Anomalous scaling laws in multifractal objects," *Phys. Rep.* **156**, 147 (1987).

<sup>4</sup>A. Crisanti, M. H. Jensen, G. Paladin, and A. Vulpiani, "Predictability of

velocity and temperature fields in intermittent turbulence," *J. Phys. A* **26**, 6943 (1993).

<sup>5</sup>A. Crisanti, M. H. Jensen, G. Paladin, and A. Vulpiani, "Intermittency and predictability in turbulence," *Phys. Rev. Lett.* **70**, 166 (1993).

<sup>6</sup>G. Paladin and A. Vulpiani, "Predictability in spatially extended systems," *J. Phys. A* **27**, 4911 (1994).

<sup>7</sup>E. Aurell, G. Boffetta, A. Crisanti, G. Paladin, and A. Vulpiani, "Predictability in systems with many characteristic times: The case of turbulence," *Phys. Rev. E* **53**, 2337 (1996).

<sup>8</sup>E. Aurell, G. Boffetta, A. Crisanti, G. Paladin, and A. Vulpiani, "Growth

- of non-infinitesimal perturbations in turbulence,” *Phys. Rev. Lett.* **77**, 1262 (1996).
- <sup>9</sup>C. E. Leith, “Atmospheric predictability and two-dimensional turbulence,” *J. Atmos. Sci.* **28**, 145 (1971).
- <sup>10</sup>C. E. Leith and R. H. Kraichnan, “Predictability of turbulent flows,” *J. Atmos. Sci.* **29**, 1041 (1972).
- <sup>11</sup>O. Metais and M. Lesieur, “Statistical predictability of decaying turbulence,” *J. Atmos. Sci.* **43**, 857 (1986).
- <sup>12</sup>C. Basdevant, B. Legras, R. Sadourny, and M. Beland, “A study of barometric model flows: intermittency, waves and predictability,” *J. Atmos. Sci.* **38**, 2305 (1981).
- <sup>13</sup>J. C. McWilliams, “The emergence of isolated coherent vortices in turbulent flow,” *J. Fluid Mech.* **146**, 21 (1984).
- <sup>14</sup>H. B. Yao, N. J. Zabusky, and D. G. Dritchel, “High gradient phenomena in two-dimensional vortex interactions,” *Phys. Fluids* **7**, 539 (1995).
- <sup>15</sup>S. A. Orszag, *Studies in applied mathematics* (Cambridge University, Cambridge, 1971), Vol. 4, p. 293.
- <sup>16</sup>G. S. Patterson and S. A. Orszag, “Spectral calculations of isotropic turbulence: Efficient removal of aliasing interactions,” *Phys. Fluids* **14**, 2538 (1971).
- <sup>17</sup>S. Kida, M. Yamada, and K. Ohkitani, “Error growth in a decaying two-dimensional turbulence,” *J. Phys. Soc. Jpn.* **59**, 90 (1990).
- <sup>18</sup>D. K. Lilly, in *International School of Physics “Enrico Fermi” Turbulence and Predictability in Geophysical Fluid Dynamics and Climate Dynamics*, edited by M. Ghil, R. Benzi, and G. Parisi (North-Holland, Amsterdam, 1985).
- <sup>19</sup>K. Ohkitani, “Wave number space dynamics of enstrophy cascade in a forced two-dimensional turbulence,” *Phys. Fluids A* **3**, 1598 (1991).
- <sup>20</sup>G. F. Carnevale, J. C. McWilliams, Y. Pomeau, J. B. Weiss, and W. R. Young, “Evolution of vortex statistics in two-dimensional turbulence,” *Phys. Rev. Lett.* **66**, 2735 (1991).
- <sup>21</sup>R. Benzi, M. Colella, M. Briscolini, and P. Santangelo, “A simple point vortex model for two-dimensional decaying turbulence,” *Phys. Fluids A* **4**, 1036 (1992).
- <sup>22</sup>J. B. Weiss and J. C. McWilliams, “Temporal scaling behavior of decaying two-dimensional turbulence,” *Phys. Fluids A* **5**, 608 (1993).
- <sup>23</sup>W. H. Matthaeus, W. T. Stribling, D. Martinez, S. Oughton, and D. Montgomery, “Decaying, two-dimensional, Navier-Stokes turbulence at very long times,” *Physica D* **51**, 531 (1991).